186. Segregation of Charge in Ions of Dibenzo[*a*,*c*]naphthacene: Relation of Topology and Electronic Structure. An NMR, ESR, and ENDOR Study

by **Yoram Cohen, Yigal Fraenkel,** and **Mordecai Rabinovitz***

Department of Organic Chemistry, The Hebrew University of Jerusalem, Jerusalem 91904, Israel

and **Patrick Felder** and **Fabian Gerson***

Institut für Physikalische Chemie der Universität Basel, Klingelbergstrasse 80, CH-4056 Basel

(23.VII.90)

^{1}H- and ^{13}C-chemical shifts of the dianion of dibenzo[*a*,*c*]naphthacene (**1**) have unambiguously been assigned by 2D-NMR spectroscopy. They indicate a remarkable charge distribution, as most of the negative charge is localized on the 'anthracenic' moiety, while the 'phenanthrenic' moiety is almost neutral. Association of $\mathbf{1}^{2-}$ with alkali-metal counterions has only a minor effect on the chemical shifts. The charge partitioning in $\mathbf{1}^{2-}$, which is reproduced by $\omega\beta$ calculations in the frame of the *Hückel* model, must, thus, be considered as an intrinsic property of the $4n\pi$-electron system of $\mathbf{1}^{2-}$. It is rationalized in terms of differing energy contents of the constituent anthracenic and phenanthrenic moieties. ESR and ENDOR studies of the radical anion $\mathbf{1}^{\cdot-}$ and the radical cation $\mathbf{1}^{\cdot+}$ show that the π-charge distribution in $\mathbf{1}^{2-}$ is reflected by the π-spin distributions in the two radical ions of the alternant hydrocarbon **1**.

Introduction. – Due to their rigidity and enforced planarity, $4n\pi$-electron dianions of $(4n'+2)\pi$-conjugated hydrocarbons ($n' = n-1$) are ideal models for the study of paratropic systems [1]. Dianions of annulenoannulenes have recently been prepared and used to discriminate between different modes of π-delocalization patterns [2]. Those of simple benzenoid hydrocarbons exhibit the expected even π-charge distribution over the entire C-framework with an alternating mode along the perimeter [3]. One was, therefore, surprised to find by ^{1}H- and ^{13}C-NMR studies that the dianion of dibenzo[*a*,*c*]naphthacene (**1**) behaves, as if it were composed of two separate substructures, thus indicating a segregation within the pertinent antibonding orbital [4]. MNDO calculations of $\mathbf{1}^{2-}$ were also reported and discussed in terms of its electron-delocalization pattern [5].

The π-charge distribution in $\mathbf{1}^{2-}$ should be reflected by the π-spin distribution in the radical anion $\mathbf{1}^{\cdot-}$, because the unpaired electron in $\mathbf{1}^{\cdot-}$ occupies, in principle, the same orbital (LUMO) as the two paired electrons uptaken by the dianion $\mathbf{1}^{2-}$, and because the π-spin populations in the radical anion of an alternant hydrocarbon are diagnostic of the π-charge populations. Moreover, due to the pairing properties of the LUMO and the HOMO [6a], an analogous statement should hold for the π-spin distribution in the radical cation $\mathbf{1}^{\cdot+}$ and the π-charge distribution in $\mathbf{1}^{2-}$.

The work described in the present paper has been undertaken to shed more light on the phenomenon of the charge segregation in $\mathbf{1}^{2-}$ and the dianions of alternant hydrocarbons. Firstly, additional ^{1}H- and ^{13}C-NMR studies by 2D techniques were performed, which corroborate the previous assignments of chemical shifts to nuclei in individual positions of $\mathbf{1}^{2-}$. Secondly, the radical anion $\mathbf{1}^{\cdot-}$ and the radical cation $\mathbf{1}^{\cdot+}$ have been characterized by their

proton-hyperfine data with the use of ESR, ENDOR, and TRIPLE-resonance spectroscopy [7]. Thirdly, the dependence of the NMR chemical shifts and the ESR coupling constants on experimental conditions was investigated to assess the importance of ion pairing of the dianion $\mathbf{1}^{2-}$ and the radical anion $\mathbf{1}^{-}$ with their positively charged alkali-metal counterions.

Results. – *NMR Studies.* Reduction of **1** to the corresponding dianion was carried out with an alkali metal (Li, Na, or K) in a perdeuterated ethereal solvent ($(D_{10})Et_2O$, (D_8)THF, or (D_{10})DME (1,2-dimethoxyethane))[4]. The NMR spectra of $\mathbf{1}^{2-}$ were taken in the temperature range of 193–318 K. The ^{1}H- and ^{13}C-chemical shifts thus obtained (*Fig. 1*) are listed in *Tables 1* and *2*, respectively. Unambiguous assignments of the ^{1}H-chemical shifts were made with the use of long-range correlation spectroscopy (COSY-LR-90; *Fig. 2*), followed by selective decoupling experiments.

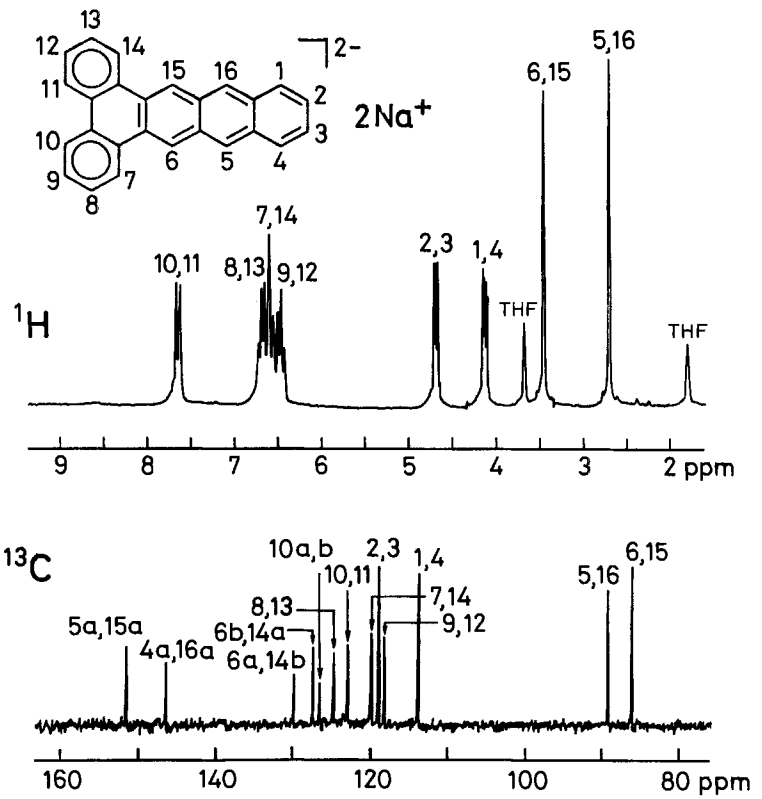

Fig. 1. *^{1}H- and ^{13}C-NMR spectra of* $\mathbf{1}^{2-}$. Solvent: (D_8)THF; temp.: 295 K. Chemical shifts relative to TMS.

Table 1. *^{1}H-NMR Chemical Shifts* [ppm] *of* $\mathbf{1}^{2-}$ [a])

Temp. [K]	Solvent	Counterion	5,16[b])	6,15	1,4	2,3	9,12	7,14	8,13	10,11
355	THF	Na^+	2.72	3.46	4.13	4.69	6.47	6.65	6.70	7.64
295	THF	Na^+	2.70	3.45	4.12	4.68	6.45	6.57	6.66	7.64
230	THF	Na^+	2.60	3.34	4.04	4.59	6.42	6.51	6.64	7.60
303	DME	Na^+	2.62	3.29	4.00	4.56	6.32	6.46	6.58	7.52
295	DME	Na^+	2.59	3.29	3.96	4.53	6.29	6.43	6.55	7.46
270[c])	DME	Na^+	2.66	3.26	3.93	4.51	6.29	6.50	6.52	7.44
290	THF	Li^+	2.65	3.42	4.11	4.67	6.33	6.51	6.58	7.54
223	THF	Li^+	2.39	3.19	3.83	4.46	6.19	6.34	6.45	7.41

[a]) Relative to TMS; experimental error: ±0.01 ppm. [b]) Position. [c]) Insoluble below this temp.

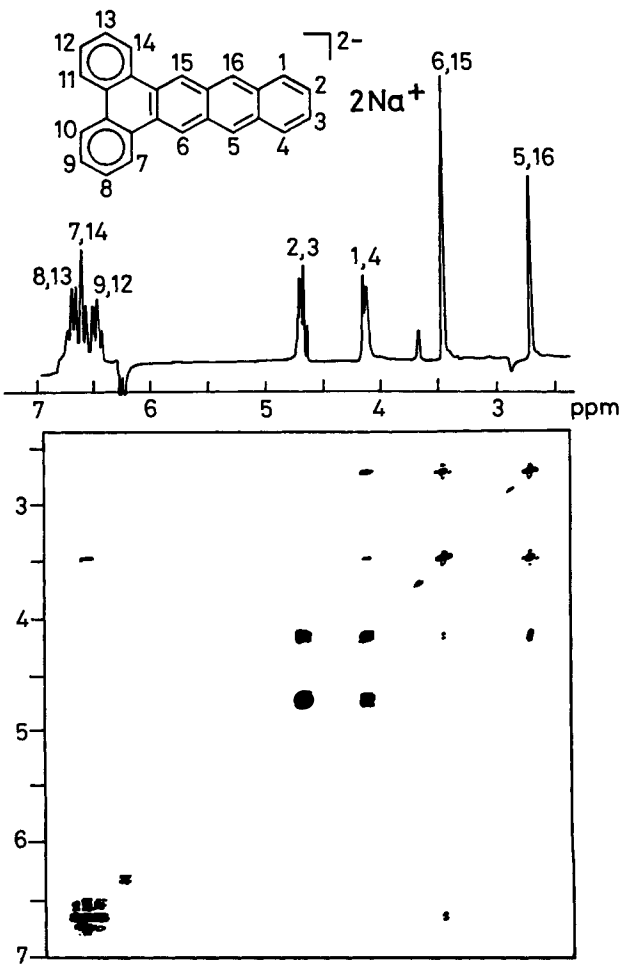

Fig. 2. *NMR-COSY-LR-90 spectrum of* $\mathbf{1}^{2-}$. Solvent and temp. as for the spectrum in *Fig. 1*. The *doublet* at 7.64 ppm, which appears folded at 6.3 ppm, is outside the displayed range (2.4–7.0 ppm).

Table 2. *^{13}C-NMR Chemical Shifts* [ppm][a]) *of* $\mathbf{1}^{2-}$

Temp. [K]	Solvent	Counterion	6,15[b])	5,16	1,4	9,12	2,3	7,14	10,11	8,13	10a,10b	6b,14a	6a,14b	4a,16a	5a,15a
313	THF	Na^+	85.48	88.70	113.20	117.70	119.00	119.30	122.36	124.18	126.04	126.82	129.34	145.97	151.01
295	THF	Na^+	85.48	88.68	113.16	117.61	118.35	119.26	122.33	124.16	125.96	126.73	129.17	145.93	150.90
230	THF	Na^+	85.94	88.90	112.90	117.40	118.10	119.28	122.30	124.08	125.61	126.35	129.29	145.94	151.05
295	DME	Na^+	87.35	90.33	112.85	116.81	117.94	119.60	122.40	123.86	125.78	126.68	130.61	147.13	152.15
270[c])	DME	Na^+	87.92	90.96	112.70	116.46	117.74	119.66	122.43	123.70	125.70	126.66	131.02	147.47	152.51
295	THF	Li^+	87.09	89.09	112.74	116.62	117.55	119.49	122.26	123.62	125.97	126.44	130.33	146.82	152.41
252	THF	Li^+	88.46	89.92	112.15	115.94	117.14	119.44	122.20	123.30	125.50	126.11	130.96	147.47	152.72
223	THF	Li^+	89.03	90.32	111.90	115.67	116.95	119.42	122.17	123.17	125.24	125.97	131.18	147.70	152.35

[a]) Relative to TMS; experimental error: ±0.05 ppm.
[b]) Position.
[c]) Insoluble below this temp.

Two cross peaks are important, namely those between the *singlet* at 3.45 ppm and the *doublet* at 6.57 ppm, and between the *singlet* at 2.70 ppm and one part of the *AA'BB'* pattern at 4.12 ppm. According to the first of these cross peaks, the *singlet* at 3.45 ppm has been attributed to H–C(6,15) and the *doublet* at 6.57 ppm to H–C(7,14); the *doublet* at 7.64 ppm is, thus, left for H–C(10,11). From the second cross peak, it can be concluded that the *singlet* at 2.70 ppm is due to H–C(5,16), and that the component of the *AA'BB'* pattern linked to this *singlet* appears at 4.12 ppm. Hence, this component has been attributed to H–C(1,4), leaving the second component of the *AA'BB'* pattern, at 4.68 ppm, for H–C(2,3). The assignment to H–C(10,11) was corroborated by measurements of the relaxation times T_1, because the *doublet* at 7.64 ppm has the shortest T_1, as expected for protons located close to each other ('bay protons'). Upon double irradiation at this signal, the *triplet* at 6.45 ppm changed into a *doublet* and has, thus, been attributed to H–C(9,12). Consequently, the *multiplet* at 6.66 ppm, the only one that has not yet been accounted for, must be due to H–C(8,13).

The ^{13}C-chemical shifts have been assigned by 2D ^{13}C,^{1}H-correlation spectroscopy; two separate experiments, one optimized for $J \approx 160$ Hz (^{1}J(C,H); *Fig. 3*) and the other for $J \approx 7.5$ Hz (upper limit of ^{3}J(C,H)) were performed.

The NMR spectra (*Figs. 1–3*) and the chemical shifts (*Tables 1* and *2*) refer to the disodium salt of $\mathbf{1}^{2-}$ which gave rise to well-resolved spectra in the whole temperature range. For the dilithium salt, the ^{1}H signals assigned to H–C(7) to H–C(14) were broad at 295 K and narrowed upon cooling to 252 K. On prolonged reduction with Li, these ^{1}H signals, as well as those of ^{13}C nuclei at C(7) to C(14) disappeared. The dipotassium salts were unstable even at low temperatures.

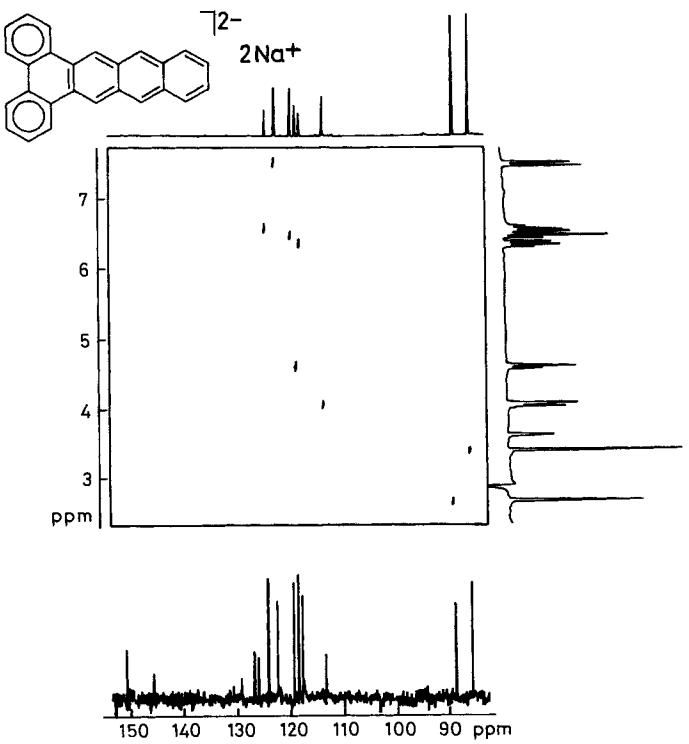

Fig. 3. *NMR ^{13}C,^{1}H-Correlation spectrum of $\mathbf{1}^{2-}$, optimized to ^{1}J(C,H) = 160 Hz.* Solvent and temp. as for the spectra in *Fig. 1*.

It is evident from *Tables 1* and *2* that variations of experimental conditions (temperature, solvent, counterion) have only a minor effect on the NMR spectra. The changes in the ^1H- and ^{13}C-chemical shifts are, in general, less than 0.3 and 3 ppm, respectively.

ESR and ENDOR Studies. The radical cation $\mathbf{1}^+$ was generated by oxidation of the neutral compound **1** with $AlCl_3$ in CH_2Cl_2, while the corresponding radical anion $\mathbf{1}^-$ was produced by reduction of **1** with K metal in DME, MTHF (2-methyltetrahydrofuran), or in a mixture of DME with HMPT (*N,N,N',N',N'',N''*-hexamethylphosphoric triamide).

The ESR spectra of $\mathbf{1}^+$ and $\mathbf{1}^-$ (*Fig. 4*) could be exactly simulated, using the hyperfine-coupling constants given in *Table 3* and derived from the positions of the proton-ENDOR

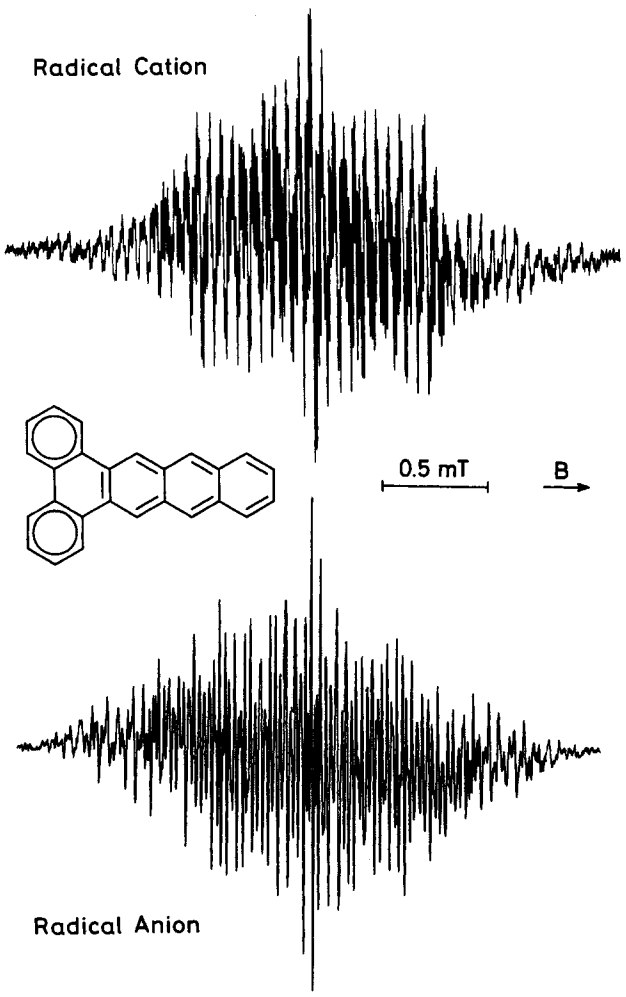

Fig. 4. *ESR spectra of* $\mathbf{1}^+$ *and* $\mathbf{1}^-$. Solvent: CH_2Cl_2 ($\mathbf{1}^+$) and 10:1 DME/HMPT ($\mathbf{1}^-$; counterion: K^+); temp. 253 ($\mathbf{1}^+$) and 213 K ($\mathbf{1}^-$). The g factor of both radical ions is 2.0027±0.0001.

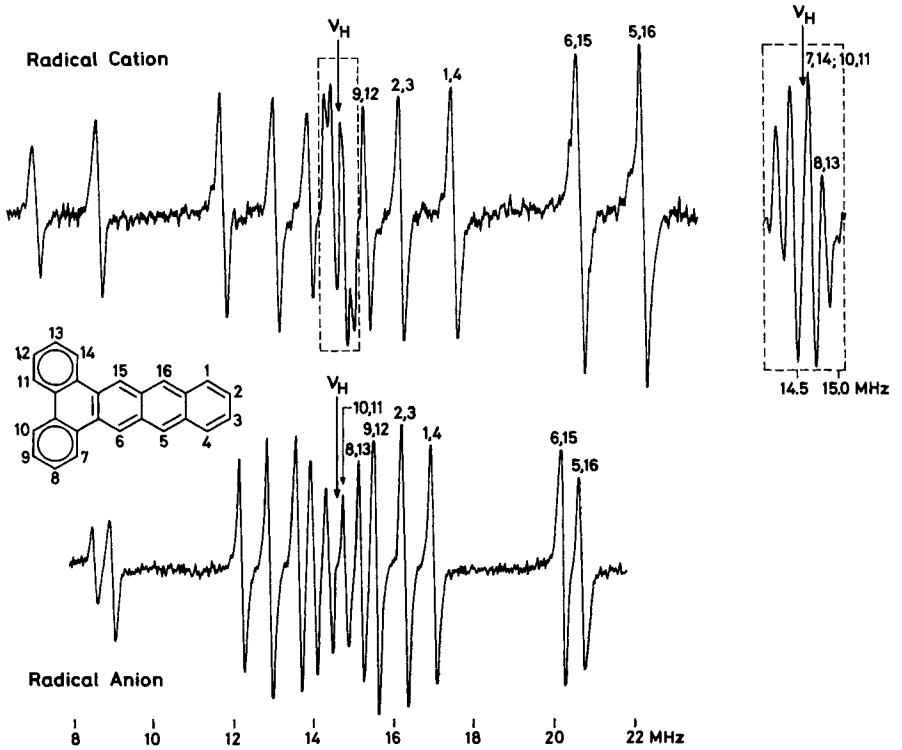

Fig. 5. *Proton-ENDOR spectra of the* $\mathbf{1}^+$ *and* $\mathbf{1}^-$. Solvent as for the spectra in *Fig. 4*; temp.: 223 ($\mathbf{1}^+$) and 193 K ($\mathbf{1}^-$). The inset at the right reproduces the central part of the spectrum of $\mathbf{1}^+$ on an expanded scale and with an improved resolution.

Table 3. *Proton-Coupling Constants,* $a_{H\mu}$[mT][a]*, of H–C(*μ*) and Calculated* π*-Spin Populations,* ρ_μ[b]*, at the Centres C(*μ*) for the Radical Ions of Dibenzo[*a,c*]naphthacene* (**1**)*, Naphthacene* (**2**)[c]*, and Anthracene* (**3**)[d]

	5,16[e])	6,15	1,4	2,3	9,12	8,13	10,11	7,14
$a_{H\mu}(\mathbf{1}^+)$	–0.544	–0.431	–0.208	–0.112	–0.052	–0.020	+0.008	+0.008
$a_{H\mu}(\mathbf{1}^-)$	–0.436	–0.407	–0.170	–0.119	–0.067	–0.043	+0.016	0.002[f])
ρ_μ	+0.214	+0.158	+0.085	+0.028	+0.011	+0.008	–0.002	0.000
	5,12[e])	6,11	1,4	2,3				
$a_{H\mu}(\mathbf{2}^+)$	–0.501	–0.501	–0.168	–0.102				
$a_{H\mu}(\mathbf{2}^-)$	–0.423	–0.423	–0.155	–0.116				
ρ_μ	+0.189	+0.189	+0.065	+0.023				
	9,10[e])	5,8	1,4	2,3				
$a_{H\mu}(\mathbf{3}^+)$	–0.653	–0.306	–0.306	–0.138				
$a_{H\mu}(\mathbf{3}^-)$	–0.535	–0.273	–0.273	–0.151				
ρ_μ	+0.248	+0.115	+0.115	+0.034				

[a]) See caption to *Fig. 4* for experimental conditions; error: ±0.002 and ±0.001 mT in $|a_{H\mu}|$ larger and smaller than 0.3 mT, respectively. [b]) *Hückel-McLachlan* procedure (λ = 1.0)[8]. [c])[12]. [d])[13]; Sign required by theory. [e]) Position μ. [f]) Estimated from ESR line-width, not observed in ENDOR spectrum; sign undetermined.

signals (*Fig. 5*). The signs allotted to these coupling constants follow from a general TRIPLE-resonance experiment [7] combined with the theoretically justified assumption that those with the largest absolute values are negative. *Table 3* also contains the π-spin populations calculated by the *Hückel-McLachlan* procedure ($\lambda = 1.0$) [8] for the proton-bearing C-atoms. The correlation between the experimental and theoretical values is sufficiently good to warrant reliable assignments of the coupling constants to the pairs of protons in $\mathbf{1}^{+}$ and $\mathbf{1}^{\cdot-}$. For the radical anion $\mathbf{1}^{\cdot-}$, the experimental values remained practically unchanged on passing from the solvent DME to MTHF or to DME/HMPT.

Formation of the radical trianion $\mathbf{1}^{3\cdot-}$ [9] upon prolonged contact of the solutions with the metallic mirror could not be observed by ESR spectroscopy.

Discussion. – The ^{1}H-NMR spectrum of $\mathbf{1}^{2-}$ (*Fig. 1*) can clearly be divided into two parts, the low-field (6.3–7.6 ppm) and the high-field one (2.5–4.7 ppm). The protons giving rise to the low-field signals belong to the angular (phenanthrenic) moiety of the π system (H–C(7) to H–C(14)), whereas those represented by the high-field signals are located in the linear (anthracenic) moiety (H–C(1) to H–C(6), H–C(15), and H–C(16)). It is noteworthy, that the high-field part in the ^{1}H-NMR spectrum of $\mathbf{1}^{2-}$ is rather close to the ^{1}H-NMR absorption region (1.5–4.0 ppm) for the dianion of anthracene [1b].

A similar partitioning effect is shown by the ^{13}C-NMR spectrum of $\mathbf{1}^{2-}$ (*Fig. 1*). The ^{13}C signals for C(7) to C(14) appear, in general, at lower field (115–125 ppm) than those for C(1) to C(4) (111–119 ppm) and, in particular, for C(5), C(6), C(15), and C(16) (85–91 ppm). As ^{13}C-chemical shifts are less prone to anisotropy effects and more sensitive to charge populations at the C-atoms than their ^{1}H counterparts [10], they provide a convincing evidence of the charge segregation in $\mathbf{1}^{2-}$. This statement is not affected by the occurrence of the low-field ^{13}C signals (145.9 and 150.9 ppm) for C(4a), C(5), C(15a), and C(16a), as such signals for quarternary C-atoms are a common feature of the dianions of 'linear' acenes like anthracene, naphthacene, and pentacene. Their appearance has been rationalized by a significant charge alternation and a low paratropicity [3].

Thus, the bulk of the π-charge population resides on the anthracenic moiety, especially on C(5,16) and C(6,15), whereas the phenanthrenic moiety is almost neutral. These conclusions are supported by $\omega\beta$-calculations in the frame of the *Hückel* model with the use of habitual parameters [11]. The total π-charge population at the twelve C-atoms C(1) to C(6), C(15), C(16), C(4a), C(5a), C(15a), and C(16a) amounts to –1.454, while that of only –0.546 is accomodated by the fourteen C-atoms C(7) to C(14), C(10a), C(10b), C(6a), C(6b), C(14a), and C(14b). The respective numbers for the radical anion $\mathbf{1}^{\cdot-}$ are approximately half as large, namely –0.742 and –0.258. This result is in accord with the two first additional electrons entering the LUMO of **1** which is largely localized on the linear (anthracenic) moiety. The calculated total charges in the radical trianion $\mathbf{1}^{3\cdot-}$ are –1.752 and –1.248 units for the anthracenic and phenanthrenic moieties, respectively. They indicate that the NLUMO (next lowest unoccupied MO) of **1**, which houses the third additional electron [9], is to a great extent confined to the angular (phenanthrenic) moiety. Unfortunately, the 'shape' of the NLUMO could not be 'verified' by experiment, as prolonged reduction of **1** with K metal failed to produce $\mathbf{1}^{3\cdot-}$ in a concentration sufficient for an ESR study. This failure may be ascribed to the high-energy level of the NLUMO which is $\alpha - 0.727\beta$ in the *Hückel* model (*vs.* $\alpha - 0.356\beta$ for the corresponding value of the

LUMO). Nevertheless, it is tempting to assume that the selective broadening in the ^{1}H- and ^{13}C-NMR spectra of $\mathbf{1}^{2-}$ upon further reduction of the dianion with Li is due to an electron exchange between $\mathbf{1}^{2-}$ and $\mathbf{1}^{3-}$ formed in low concentration, because the signals affected by the broadening belong to the nuclei in the phenanthrenic moiety (positions 7–14).

The pairing properties of the alternant hydrocarbon **1** are borne out by the similarity of the proton hyperfine coupling constants for the radical cation $\mathbf{1}^{+}$ and the radical anion $\mathbf{1}^{-}$ (*Table 3*). The somewhat larger absolute values of the most prominent coupling constants for $\mathbf{1}^{+}$ than for $\mathbf{1}^{-}$ are in line with the analogous findings for the radical ions in the acene series [6a]. There is a good correlation between the proton hyperfine data for $\mathbf{1}^{+}$ and $\mathbf{1}^{-}$ with the ^{1}H- and ^{13}C-chemical shifts for $\mathbf{1}^{2-}$, thus indicating a similar pattern of π-charge distribution. The coupling constants, which point to an almost exclusive location of the π-spin population in the linear moiety of $\mathbf{1}^{-}$ and $\mathbf{1}^{+}$, are comparable to the corresponding values for the radical ions of naphthacene [12]. However, a significant shift of this population away from the dibenzo-substituted part of the linear moiety causes the π-spin distribution in $\mathbf{1}^{-}$ and $\mathbf{1}^{+}$ to approach that in the radical ions of anthracene [13] (*Table 3*).

Association of a hydrocarbon anion such as $\mathbf{1}^{-}$ and $\mathbf{1}^{2-}$ with the positively charged alkali-metal counterion (ion pairing) [6b][14] becomes weaker by an increase in the cation-solvating power of the solvent (MTHF < THF < DME < HMPT), by a decrease in the size of the counterion ($Cs^+ > Rb^+ > K^+ > Na^+ > Li^+$), and by lowering the temperature. The ^{13}C-NMR chemical shifts of $\mathbf{1}^{2-}$ for the most highly charged positions (C(5), C(6), C(15), and C(16)) follow the expected trends. On going from THF to DME, on replacing Na^+ by Li^+, and on cooling the solution, the pertinent ^{13}C signals move to lower field (*Table 2*), because the counterion becomes less effective in polarizing the charge distribution. However, these shifts induced by the ion pairing are one order of magnitude less than those incurred by the charge partitioning. An analogous statement holds with respect to the ^{1}H-NMR chemical shifts of $\mathbf{1}^{2-}$. Likewise, ion pairing has no marked effect on the proton-coupling constants in the ESR spectrum of $\mathbf{1}^{-}$, as indicated by their being almost independent on the solvating power of the solvent.

The charge partitioning is, therefore, an intrinsic property of some $4n\pi$-electron dianions of alternant hydrocarbons such as **1**, and its occurrence depends on the topology of the charged π system. The question is what is the cause of this surprising distribution mode which has also been observed for the dianions of structurally related polyheterocyclic systems [15]. Naively, it could be assumed that the best pattern of the charge delocalization is the one in which the changes are spread over the entire system, thus reducing the *Coulombic* repulsion. As suggested previously [4], the rationale for the deviation from this pattern encountered with $\mathbf{1}^{2-}$ (and also prevailing in $\mathbf{1}^{+}$ and $\mathbf{1}^{-}$) is the energy content involved in the different modes of charge distribution. Relevant are the relative energy changes on passing from a constituent $(4n'+2)\pi$ moiety to the corresponding $4n\pi$-one. The destabilization occurring upon formation of the dianion, and also that of radical ions, is larger for the angular than for the linear moiety. (In the case of **1**, *e.g.*, the *Hückel* energies of the frontier MO's are $\alpha \pm 0.414\beta$ for anthracene and $\alpha \pm 0.605\beta$ for phenanthrene; the positive and negative sign referring to the HOMO and LUMO, respectively.) It has been proposed [4] that the ions would have much more 'to loose', if most of the charge were directed toward the angular instead of linear moiety. In $\mathbf{1}^{2-}$, a doubly charged 'phenanthrenic' and an almost neutral 'anthracenic' moiety should be energetically less

favourable, as such a charge distribution pattern involves more pronounced paratropic contributions [16].

Experimental. – *Dibenzo[a,c]naphthacene* (**1**). The following improved procedure was applied to the preparation of this compound. 2,3-Di(bromomethyl)naphthalene (0.05M) was reacted with triphenylphosphine (0.12M) in 150 ml of DMF at 80–90°. After 1 h, a white precipitate began to form. The reaction was carried on for 20 h. The mixture was then cooled down to r.t. and the solvent evaporated. Recrystallization afforded the phosphonium salt (95% yield). This was dissolved in 150 ml of CH_2Cl_2 and, after addition of phenanthrenequinone (0.01M), the org. soln. was reacted with 5N aq. LiOH prepared by dissolving the metal in H_2O. The two-phase system was stirred for 72 h. 200 ml of H_2O were added to the mixture, and the product was extracted (3 ×, CH_2Cl_2). The org. layer was dried ($MgSO_4$), and the solvent was filtered and evaporated. The product **1** was recrystallized (2 ×) from toluene. M.p. 207–209° ([17]: 205°)

Reduction of **1** to its dianion $\mathbf{1}^{2-}$ with a Li or Na wire or a K chip in (D_8)THF, (D_{10})DME, or (D_{10})Et_2O was carried out as described in [4a]. The concentration was in the range $2 \cdot 10^{-3}$–$9 \cdot 10^{-2}$ mol/dm^3. After each experiment, the soln. of $\mathbf{1}^{2-}$ was quenched with O_2 or MeI, and the intact neutral compound **1** could be regenerated. Starting from **1**, preparation of the radical cation $\mathbf{1}^{+}$ with $AlCl_3$ in CH_2Cl_2 and of the radical anion $\mathbf{1}^{-}$ with K in DME, MTHF, or DME/HMPT followed the well established procedures [6c][18].

Instrumental. NMR studies were performed on a *Bruker-WP-200-SY* spectrometer, equipped with a pulse programmer and an *Aspect-2000* computer. For 2D-NMR experiments use was made of standard DISN85 programs (*Bruker Physik*). ESR spectra were taken on a *Varian-E9* instrument, while a *Bruker-ESP-300* spectrometer served for ENDOR and TRIPLE-resonance studies.

This work was supported by a grant from the *U.S.-Israel Binational Science Foundation* and the *Schweizerischer Nationalfonds zur Förderung der wissenschaftlichen Forschung*. Financial assistance by *Ciba-Geigy AG, Sandoz AG,* and *F. Hoffmann-La Roche & Co. AG*, Basel, is acknowledged. *M.R.* thanks Prof. *A.Y. Meyer*, Jerusalem, for fruitful discussions.

REFERENCES

[1] a) M. Rabinovitz, Y. Cohen, *Tetrahedron* **1988**, *44*, 6957; b) A. Minsky, A. Y. Meyer, R. Poupko, M. Rabinovitz. *J. Am. Chem. Soc.* **1983**, *105*, 2164; c) M. Rabinovitz, Y. Cohen, A.C.S. Advances in Chemistry Series No. 217, 'Chemistry of Polynuclear Aromatics', Ed. L. B. Ebert, 1987.
[2] K. Müllen, W. Huber, T. Meul, M. Nakagawa, M. Iyoda, *J. Am. Chem. Soc.* **1982**, *104*, 5403.
[3] Y. Cohen, J. Klein, M. Rabinovitz, *J. Am. Chem. Soc.* **1988**, *110*, 4634.
[4] a) A. Minsky, M. Rabinovitz, *J. Am. Chem. Soc.* **1984**, *106*, 6755; b) M. Rabinovitz, *Topics Curr. Chem.* **1988**, *146*, 99.
[5] C. Glidewell, D. Lloyd, *Chem. Scr.* **1986**, *26*, 373; *Tetrahedron* **1984**, *40*, 4455.
[6] F. Gerson, 'High-Resolution ESR Spectroscopy', Wiley, New York, and Verlag-Chemie, Weinheim, 1970; a) Chapt. 2.1; b) Appendix A.2.2; c) Chapt. 1.4.
[7] H. Kurreck, B. Kirste, W. Lubitz, 'Electron Nuclear Double Resonance of Radicals in Solution', VCH Publishers, New York, 1988, Chapt. 2.
[8] A.D. McLachlan, *Mol. Phys.* **1960**, *3*, 233.
[9] F. Gerson, W. Huber, *Acc. Chem. Res.* **1987**, *20*, 85.
[10] a) R. Schaeffer, W. G. Schneider, *Can. J. Chem.* **1963**, *41*, 966; b) B. Eliasson, U. Edlund, K. Müllen, *J. Chem. Soc., Perkin Trans. 2* **1986**, 937.
[11] G. V. Boyd, N. Singer, *Tetrahedron* **1966**, *22*, 3383.
[12] P. Felder, F. Gerson, unpublished results.
[13] J. R. Bolton, G. K. Fraenkel, *J. Chem. Phys.* **1964**, *40*, 3307.
[14] a) 'Ions and Ion Pairs in Organic Reactions', Ed. M. Szwarc, Wiley Interscience, New York, Vol. I, 1970, Vol. II, 1972; b) R. N. Young, *Prog. Nucl. Magn. Reson. Spectrosc.* **1978**, *12*, 261.
[15] Y. Cohen, A. Y. Meyer, M. Rabinovitz, *J. Am. Chem. Soc.* **1986**, *108*, 7039.
[16] C. W. Haigh, R. B. Maillion, *Prog. Nucl. Magn. Reson. Spectrosc.* **1979**, *13*, 303.
[17] E. Clar, 'Polycyclic Hydrocarbons', Academic Press, London, 1964, Vol. 1.
[18] W. B. Forbes, P. D. Sullivan, *J. Am. Chem. Soc.* **1966**, *88*, 2862.